


Role of the Environment in Quenching the Production of H_3^+ from Dicationic Clusters of Methanol

Enliang Wang^{1,*}, Xueguang Ren^{2,1,†} and Alexander Dorn^{1,‡}

¹Max-Planck-Institut für Kernphysik, Saupfercheckweg 1, 69117 Heidelberg, Germany

²School of Physics, Xi'an Jiaotong University, Xi'an 710049, China

 (Received 15 October 2020; revised 8 January 2021; accepted 9 February 2021; published 10 March 2021)

Ionization and subsequent isomerization of organic molecules has been suggested as an important source of trihydrogen H_3^+ cations in outer space. The high interest in such reactions has initiated many experimental and theoretical studies for various molecules. Here, we report measurements as well as *ab initio* molecular dynamics simulations on the fragmentation of dicationic methanol monomers and clusters ionized by low-energy (90 eV) electrons. Experimentally, for dicationic monomers, a fragmentation channel for the formation of H_3^+ in coincidence with a COH^+ cation is observed. The simulations show that an intermediate neutral H_2 is formed in the first step, and its roaming around the dication ends in the formation of H_3^+ . The entire reaction takes about 100–500 fs. The calculated kinetic energy release for the $\text{H}_3^+ + \text{COH}^+$ ion pair is in excellent agreement with the experimental result. In contrast, for the dicationic clusters, due to the possibility of distributing the two charges onto different molecules, several fast dissociation channels occur and suppress the roaming of H_2 and formation of H_3^+ . The present Letter suggests that the quenching of H_3^+ formation by the chemical environment is a general phenomenon in dicationic clusters of organic molecules.

DOI: [10.1103/PhysRevLett.126.103402](https://doi.org/10.1103/PhysRevLett.126.103402)

The trihydrogen H_3^+ cation is the most prevalent molecular ion in interstellar space and plays an important role in astrochemistry due to its high activity in initiating various chemical reactions in interstellar clouds [1]. H_3^+ can be regarded as a universal proton donor to reactants through the proton hopping reaction [2], $\text{H}_3^+ + \text{X} \rightarrow \text{HX}^+ + \text{H}_2$. Once protonated, the charged unit becomes far more active than the neutral one and, thereby, chains of reactions are launched that produce larger and more diverse molecules [3,4].

It is known that H_3^+ can be formed efficiently by collisions involving H_2^+ ions and neutral hydrogen gas, i.e., $\text{H}_2^+ + \text{H}_2 \rightarrow \text{H}_3^+ + \text{H}$. Molecular dynamical studies suggest an alternative mechanism concerning ionization and fragmentation of organic compounds that can produce H_3^+ via isomerization processes [5–23]. For example, formation of H_3^+ due to the charge separation process of the methanol dication has been reported in experiments for photoionization by Eland *et al.* [5,6] and for highly charged ion collisions by De *et al.* [7]. Recently, experiments using intense laser fields have been performed to study the H_3^+

formation dynamics in the dissociative ionization of several organic molecules, like methanol, ethanol, 1-propanol, 2-propanol tert-butanol, ethylene glycol, ethane, and acetone, etc., [8–21]. Molecular dynamics simulations revealed a two step mechanism for H_3^+ formation, which is started by forming an intermediate neutral H_2 . This stabilizes the dication and allows the H_2 molecule to roam around the ion until a proton is transferred to form H_3^+ and COH^+ which undergo Coulomb explosion. Time-resolved experiments confirmed that the entire reaction takes about 100 fs for formation of H_3^+ in the methanol dication [18–20].

Previous studies have focused mainly on the target of isolated molecules in the gas phase. In recent years, weakly bonded complexes are receiving increasing attention in many interdisciplinary studies as they form the links between the isolated molecules in the gas phase and the condensed phases of matter [24,25]. Molecular complexes are considered to play an important role in the chemistry of the interstellar medium, in particular, in dense and cold molecular clouds and, also, at the higher densities and temperatures found in planetary atmospheres [26–28]. Also, the methanol-based reactions are relevant to astrochemistry since methanol is readily observed in a wide range of interstellar media [29] in which all of the molecules are being bombarded by high-energy radiation and, in particular, a large number of secondary electrons [30]. Irradiation of astrophysical ice analogs (low-temperature molecular complexes like H_2O , CO , CO_2 ,

Published by the American Physical Society under the terms of the [Creative Commons Attribution 4.0 International license](https://creativecommons.org/licenses/by/4.0/). Further distribution of this work must maintain attribution to the author(s) and the published article's title, journal citation, and DOI. Open access publication funded by the Max Planck Society.

NH_3 , and CH_3OH) by ultraviolet (UV) photons in the laboratory has produced a suite of organic molecules including amino acids, amphiphiles, quinones, and nucleobases [31]. The protonation of widespread methanol to form CH_3OH_2^+ is thought to be central to understanding how molecules of even greater complexity could be formed in abundance [4,32].

In this Letter, we discuss the influence of a chemical environment on the formation of H_3^+ from methanol. We study how the low-energy electron (90 eV) initiated double ionization dynamics of methanol monomers changes in going to dimers and larger clusters. The decisive aspect, here, is that, if a dication in its electronic ground state is placed within a dimer or cluster, the whole system is in an electronically excited state. This is because, for the ground state, the charges are shared by two or more molecules such that the Coulomb (repulsion) energy is reduced as compared to a situation where both charges are on one center. As a result, new reaction channels are open where charges, i.e., electrons or protons but, also, neutrals are transferred between the constituents of the cluster. Our experimental results and accompanying *ab initio* molecular dynamics (AIMD) simulations show that direct Coulomb explosion (CE) and the hydrogen or proton transfer mediated Coulomb explosion [33,34] (for general discussion, we name both PTMCE) processes occur in the dicationic clusters, and these outperform the formation of H_3^+ .

The experiments were performed using a multiparticle coincident momentum spectrometer (reaction microscope) combined with a pulsed electron beam [35–37]. The methanol clusters were generated by a supersonic gas expansion of helium gas (1 bar) seeded with methanol vapor. The mixed gas expanded into the vacuum chamber through a 30 μm nozzle and was collimated by two skimmers with aperture diameters of 200 μm located at about 3 mm and 2 cm downstream from the nozzle, respectively. All of the methanol reservoir, gas line, and nozzle were kept at room temperature. The pulsed electron beam ($E_0 = 90$ eV) is emitted from an electron gun consisting of a tantalum photocathode which is irradiated by UV light ($\lambda = 266$ nm) with 0.5 ns duration and electrostatic focusing lens elements. The electron beam is crossed with the gas jet causing ionization. The outgoing electrons and ions are extracted by uniform electric and magnetic fields with magnitudes of 25 V cm^{-1} and ~ 7 Gauss, respectively, and are detected by two time- and position-sensitive delay line detectors. The momentum vectors and, consequently, kinetic energies of the outgoing charged particles can be determined from the measured time of flight and positions of the particles hitting the detectors. In the present experiment, triple coincidences of two fragment ions and one outgoing electron were recorded. This yields the kinetic energy release (KER) of the two fragment ions and the projectile energy loss related to the ion pair.

The calculations were carried out with the Car-Parrinello molecular dynamics [38] and Gaussian16 [39] packages. For isolated methanol (M), we consider the removal of two electrons from the outermost orbital of the molecule, i.e., the electronic ground state of the molecular dication (M^{++}). As stated above, for dimers (clusters), there can be two electronic configurations of the initial dication. One is the removal of the outermost electron from each of the molecules, i.e., the charges are shared by two molecules. This corresponds to the electronic ground state of the dimer dication ($\text{M}^+ \cdot \text{M}^+$). In the other case, the two charges are initially located on one molecule of the methanol dimer ($\text{M}^{++} \cdot \text{M}$). Our further analysis (see Supplemental Material [40]) shows that the charge-localized state will convert to the charge-delocalized states of $\text{M} \cdot \text{H}^+ \cdot (\text{M}-\text{H})^+$ or $\text{M}^+ \cdot \text{M}^+$ through the ultrafast proton transfer [41] or charge transfer mechanisms [42]. The calculated potential energy curves show that the proton transfer channel in the dicationic dimer of methanol is almost barrierless if two electrons are removed from the outer valence orbitals of the proton donor site of the dimer.

The charge transfer is analyzed using the classical-over-the-barrier model (see Supplemental Material [40]) in which an electron of the neutral can be directly abstracted by the doubly charged group if the distance of two moieties is less than the critical distance [42]. This is fulfilled in the present case where the intermolecular carbon-carbon distance (~ 4.35 Å, the largest distance between two heavy atoms in the dimer) is smaller than the critical distance for the methanol dimer (~ 5.1 Å). Once the charge is transferred, the electronic configuration decays to the charge-delocalized state of the dimer dication. Thereby, in our molecular dynamics calculations of methanol dimers and larger clusters, we consider the charge-delocalized $\text{M}^+ \cdot \text{M}^+$ dication as the initial state. In principle, this state can also be produced by other ionization mechanisms like the intermolecular Coulombic decay [43–45] or by sequential ionization where the projectile electron successively kicks out one electron from each molecule of the methanol dimer and, thus, also leads to the $\text{M}^+ \cdot \text{M}^+$ state. This is supported by the measured onset of the projectile energy loss at about 26 eV for the $\text{M} \cdot \text{H}^+ + \text{M}_2 \cdot \text{H}^+$ fragmentation channel as shown in Fig. 1(b) which is significantly less than the double ionization energy (~ 32 eV) [46] of the methanol molecule.

In our AIMD simulations, the equilibrium geometries of the neutral molecule and clusters were first optimized, and then, an equilibration run was performed using a Nosé-Hoover chain at a temperature of 25 K which simulates the vibration of the neutral methanol molecule and clusters. The temperature in the simulation is very close to the most probable experimental one (20 K). The experimental temperature is determined by a kinematically complete coincidence of two outgoing electrons with M^+ (see Supplemental Material [40]). The initial atomic

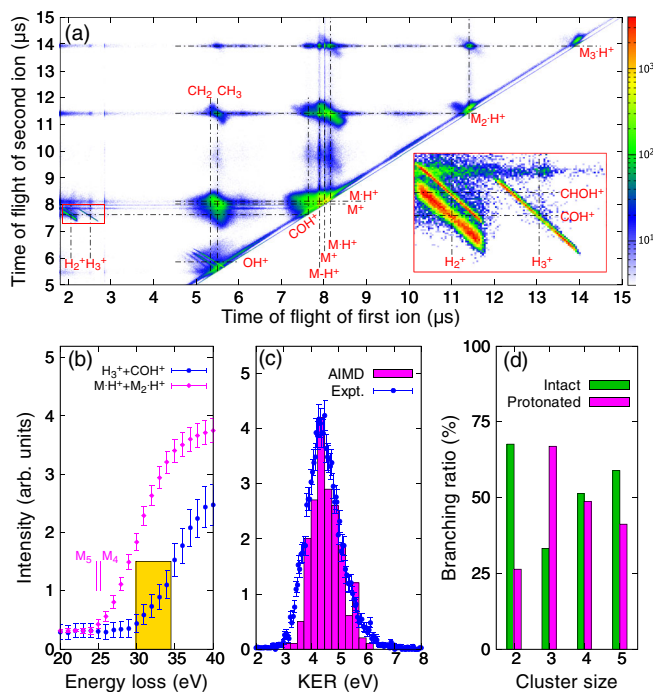


FIG. 1. (a) Time correlation map of two ions in which the time of flight of the second ion is plotted against the first one. (b) The projectile energy loss of channels for H_3^+ emission, and $M^+H^+ + M_2^+H^+$ coincidence. The experimental data are normalized by putting the base between 20 and 25 eV at the same level. M_4 and M_5 mean tetramer and pentamer, respectively. The yellow shadow marks the Franck-Condon region of double ionization of methanol monomer. (c) Experimental and simulated kinetic energy release of the $H_3^+ + COH^+$ channel. (d) The simulated branching ratio of the number of dissociation channels into intact and protonated species as a function of cluster size.

configuration (positions and velocities) for AIMD simulation is taken every 2.4 fs after a long equilibration run (5 ps). We start the dynamical simulation from the obtained initial atomic configuration and a vertical transition to the electronic ground state of the doubly charged methanol molecule (M^{++}) or dimer or larger cluster ($M^+ \cdot M^+$). Here, we consider the electronic singlets in the calculations due to the minor contribution of the triplet states in the dications [21]. Dynamical simulations were performed under the extended Lagrangian molecular dynamics scheme in which the so-called atom-centered density matrix propagation [47–49] and the density functional theory (DFT) at B3LYP/cc-pVDZ level are adopted.

The experimental time-correlation map between two fragment ions is presented in Fig. 1(a). Several fragmentation channels are identified, i.e., H_2^+/COH^+ , $H_2^+/CHOH^+$, H_3^+/COH^+ and CH_n^+/OH^+ , $CH_n^+/M_n \cdot H^+$ ($n = 1, 2, 3$) and the coincidence patterns between two of the protonated species $M_n \cdot H^+$ ($n = 1, 2, 3$). We observe only one fragmentation channel for the emission of H_3^+ which can be more clearly seen from the zoom-in view on the right bottom of Fig. 1(a). The sharp correlation line between H_3^+

and COH^+ means that two ions are ejected back to back with momenta of equal magnitude. This is an indication of a pure two-body dissociation channel from the methanol dication (M^{++}). If there are some undetected neutral fragments, the correlation line will become broader, as is seen for the $H_2^+ + COH^+$ channel with one neutral H loss from M^{++} . This also rules out any contributions of H_3^+ from the dicationic fragmentation of methanol clusters with the loss of neutral species or molecular evaporation. We observed an abundant production of protonated species from the dicationic clusters. The production of such species is also observed in our AIMD simulations, although it must be mentioned that, here, the initial state is $M^+ \cdot M^+$ and neutral hydrogen transfer is required. As shown in Fig. 1(d), about 25% of our simulated trajectories of dicationic dimers end up with the protonation channel. This value is increased to about 67%, 49%, and 41% for trimers, tetramers, and pentamers, respectively.

The mechanism for H_3^+ formation from the M^{++} dication is consistent with the previous studies of methanol [19,20,22]. In brief, an ultrafast (less than 15 fs) double-H migration takes place in the first step and forms a neutral H_2 molecule which undergoes a roaming process and a proton transfer from CH_2O^{++} to H_2 producing H_3^+ . The center of mass (COM) distances between the H_3^+ and COH^+ fragments as a function of time are shown in Figs. 2(a) and 2(b) for the abstraction of the proton from the

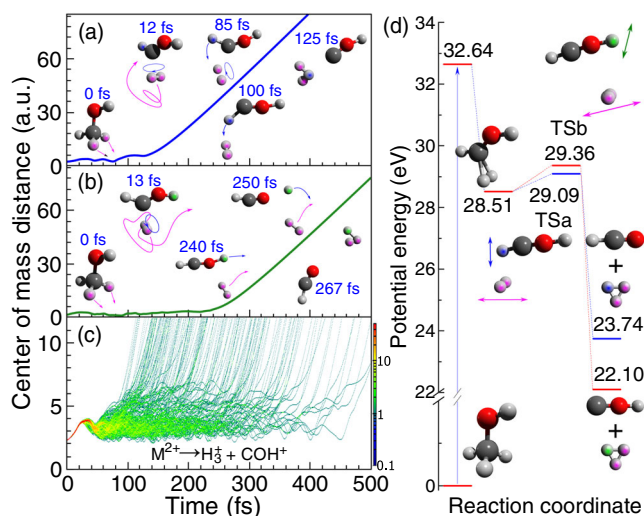


FIG. 2. Calculated center-of-mass distances between H_3^+ and HCO^+ as a function of time (left column) and potential energies (right column) for the Coulomb explosion ($H_3^+ + HCO^+$) dynamics induced by double ionization of the methanol molecule. (a) and (b) Selected trajectories for H_2 roaming followed by abstracting a proton from carbon and hydroxyl sites, respectively. The double-H migration and proton abstraction are marked by the short curved arrows. The roaming paths are marked by the long curved arrows. (c) All simulated trajectories of $H_3^+ + HCO^+$. The ratio of $H_3^+ + HCO^+$ channel to all of the trajectories is 193:2000. (d) Energy levels for the transition states.

carbon and hydroxyl sites, respectively. In Fig. 2(b), the H_2 roaming path is longer than that in Fig. 2(a) due to the larger initial distance between H_2 and the hydroxyl. This leads to an even longer time (~ 260 fs) for formation of H_3^+ by abstracting a proton from the hydroxyl site. Additionally, it is shown in Fig. 2(d) that the potential energy barrier for the transition state (TS) encountered in the channel for proton abstraction from the hydroxyl site is slightly higher (0.85 eV) than that from the carbon site (0.58 eV), meaning a higher rate for proton abstraction from the carbon site. These values were calculated by DFT using the ω B97XD functional with cc-pVTZ basis set and corrected by zero point energy. The present simulations are justified by comparison with the experimental data. As can be seen from Fig. 1(c), the calculated KER spectrum for the $H_3^+ + COH^+$ channel is in excellent agreement with experiment both in shape and peak position (~ 4.3 eV) of the KER. From all calculated trajectories [Fig. 2(c)], we find that H_3^+ can appear from about 100 to ~ 500 fs which is also in good agreement with the time-resolved measurements on methanol molecules [18–20].

Now, we focus on the fragmentation dynamics of dicationic dimers ($M^+ \cdot M^+$). Generally, there are two mechanisms initiating the fragmentation processes, i.e., the direct CE and the PTMCE leading to the protonated and deprotonated species. The COM distances between different species are presented in Figs. 3(a)–3(c). The curves for the direct CE channel [Fig. 3(a)] exhibit monotonically

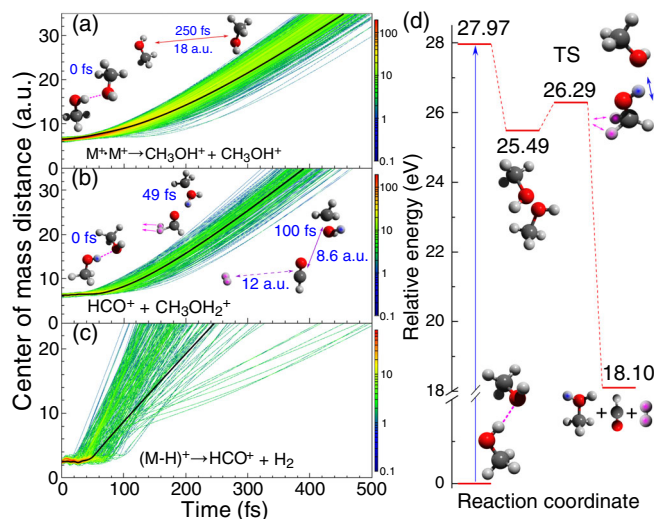


FIG. 3. Calculated center-of-mass distances as a function of time (left column) and potential energies (right column) for the dicationic fragmentation of methanol (M) dimers. (a) Direct Coulomb explosion: $M^+ \cdot M^+ \rightarrow M^+ + M^+$. (b) The fragment ions of $HCO^+ + M \cdot H^+$ from the hydrogen or proton transfer mediated Coulomb explosion process. (c) Further dissociation of the deprotonated methanol: $(M-H)^+ \rightarrow HCO^+ + H_2$. (d) Energy levels for the transition states. The molecular structures in (a) and (b) are taken from the trajectory marked by the solid (black) curves.

increasing distance with increasing time, meaning that the system will dissociate into two intact M^+ ions once the $M^+ \cdot M^+$ dication is formed. For PTMCE, the dissociation starts at about 50 fs [Fig. 3(b)] at which the $M \cdot H^+ \cdot (M-H)^+$ dicationic state is formed. In this process, a neutral H_2 is formed in the deprotonated methanol $(M-H)^+$. This can be seen from the vibration mode of the TS corresponding to the PTMCE channel shown in Fig. 3(d). The $(M-H)^+$ cation dissociates into HCO^+ and H_2 at the time range about 20–80 fs [Fig. 3(c)]. The fast separation inhibits the roaming mechanism of H_2 in $(M-H)^+$. These results indicate that the direct CE and PTMCE processes in the dicationic dimers are faster than the roaming mechanism of H_2 and quench the production of H_3^+ .

Figure 4 shows the dynamical simulations for dicationic trimers (top row), tetramers (middle row), and pentamers (bottom row). These calculations reveal essentially similar mechanisms to those involved in the fragmentation of dicationic dimers. It can be seen from the curves showing the intermolecular oxygen-oxygen distances as a function of time in the left column of Fig. 4 that the ultrafast (< 100 fs) dissociation channels (direct CE and PTMCE) occur in the dicationic clusters. For PTMCE, the hydrogen or proton transfer can be complete within about 60 fs (right column in Fig. 4) and then the dissociation starts by forming protonated and deprotonated species. Again, a neutral H_2 can be formed in the deprotonated $(M-H)^+$. As the two charges are delocalized over the whole molecular cluster, the reaction between the neutral H_2 and the remaining charged species becomes less efficient due to

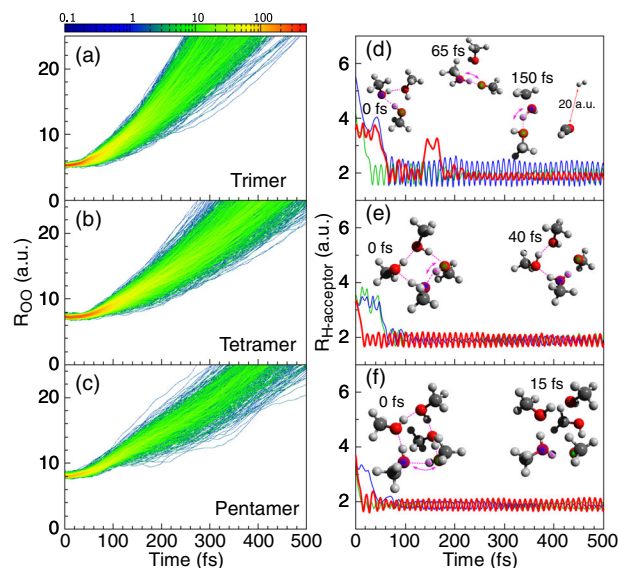


FIG. 4. Intermolecular oxygen-oxygen distances (left column) and the migrated hydrogen and acceptor distances (right column) as a function of time for the dicationic fragmentation of trimers (a) and (d), tetramers (b) and (e), and pentamers (c) and (f). In the molecular structures, the hydrogen donor, acceptor, and migrated hydrogen are shown by green, blue, and violet color, respectively.

the reduced charge density. Therefore, instead of roaming around the system, the neutral H_2 will directly fly away and, thereby, quench the formation of H_3^+ , see, e.g., the time-resolved molecular structures in Fig. 4(d). Overall, the present results indicate that the formation of H_3^+ from the dicationic clusters is suppressed by the competing processes of direct CE and PTMCE. It is also to be noted that the dicationic clusters produce a large number of protonated species and other radical ions [see Fig. 1(d)], which can be important for the chemical reactions forming complex molecules in interstellar space [2–4,32].

Furthermore, we calculated the rotational (E_{rot}) and vibrational (E_{vib}) energies of H_3^+ and CH_3OH_2^+ produced from the dications of the methanol monomer (Fig. 2) and the dimer (Fig. 3), respectively. The averaged energies are $E_{\text{rot}} \sim 0.2$ eV and $E_{\text{vib}} \sim 1.0$ eV for H_3^+ and $E_{\text{rot}} \sim 0.16$ eV and $E_{\text{vib}} \sim 2.15$ eV for CH_3OH_2^+ . Considering the energies of the normal vibrational modes (see the Supplemental Material [40]), this indicates that, while H_3^+ is produced mainly in the lowest vibrational quantum numbers in CH_3OH_2^+ , significantly higher vibrational states are excited. These results can help to examine the infrared spectral lines of interstellar molecular species, in particular, for the identification of CH_3OH_2^+ [4].

In summary, we presented a combined experimental and theoretical study on trihydrogen H_3^+ formation from dicationic fragmentation of methanol monomers and clusters ionized by low-energy (90 eV) electrons. Experimentally, we identified a single reaction for the production of H_3^+ , i.e., the $\text{H}_3^+ + \text{COH}^+$ fragmentation channel. Further analysis of the data indicates that this channel can be solely attributed to the double ionization of methanol monomers, and the fragmentation of dicationic methanol clusters does not contribute. This is supported by the *ab initio* molecular dynamics simulations. For the monomer, our calculations show that, at first, an intermediate neutral H_2 molecule is formed in the methanol dication, and its subsequent roaming in the vicinity of the system causes the formation of H_3^+ by abstracting a proton within the time range 100–500 fs. This is consistent with published time-resolved measurements on the double ionization of the methanol molecule [18–20].

For the fragmentation dynamics of small dicationic clusters ranging from dimers up to pentamers, we found that the dissociation processes occur primarily through direct Coulomb explosion and hydrogen or proton transfer mediated Coulomb explosion. Both CE and PTMCE are faster than 100 fs and, thereby, outperform the roaming mechanism and quench the formation of H_3^+ . The dicationic clusters dissociate into intact, protonated, and deprotonated species. It is shown that a neutral H_2 can also be formed in the deprotonated species, it will directly recede from the system, instead of roaming in the vicinity to form H_3^+ . The methanol molecule within a chemical environment has the possibility to distribute its charge to neighbors,

leading to fast dissociation pathways and, thus, suppressing H_3^+ formation. We suggest that the quenching of H_3^+ formation by the chemical environment is a general phenomenon in dicationic clusters of organic molecules. Indeed, our further experiments indicate that it may also occur in ethanol clusters (see the Supplemental Material [40]). This study provides new insight on the dynamics of dicationic methanol clusters and expands our understanding of the formation mechanism of H_3^+ and CH_3OH_2^+ in the interstellar medium.

This work was jointly supported by the National Natural Science Foundation of China under Grants No. 11974272 and No. 11774281 and by the Deutsche Forschungsgemeinschaft (DFG) project. E. W. acknowledges a fellowship from the Alexander von Humboldt Foundation.

*enliang@phys.ksu.edu; Present address: J. R. Macdonald Laboratory, Physics Department, Kansas State University, Manhattan, Kansas 66506, USA.

†renxueguang@xjtu.edu.cn

‡alexander.dorn@mpi-hd.mpg.de

- [1] S. Miller, J. Tennyson, T. R. Geballe, and T. Stallard, *Rev. Mod. Phys.* **92**, 035003 (2020).
- [2] T. Oka, *Proc. Natl. Acad. Sci. U.S.A.* **103**, 12235 (2006).
- [3] D. Smith, *Chem. Rev.* **92**, 1473 (1992).
- [4] B. A. McGuire, O. Asvany, S. Brünken, and S. Schlemmer, *Nat. Rev. Phys.* **2**, 402 (2020).
- [5] J. Eland and B. Treves-Brown, *J. Mass Spectrom. Ion Processes* **113**, 167 (1992).
- [6] J. H. D. Eland, *Rapid Commun. Mass Spectrom.* **10**, 1560 (1996).
- [7] S. De, J. Rajput, A. Roy, P. N. Ghosh, and C. P. Safvan, *Phys. Rev. Lett.* **97**, 213201 (2006).
- [8] Y. Furukawa, K. Hoshina, K. Yamanouchi, and H. Nakano, *Chem. Phys. Lett.* **414**, 117 (2005).
- [9] T. Okino, Y. Furukawa, P. Liu, T. Ichikawa, R. Itakura, K. Hoshina, K. Yamanouchi, and H. Nakano, *J. Phys. B* **39**, S515 (2006).
- [10] T. Okino, Y. Furukawa, P. Liu, T. Ichikawa, R. Itakura, K. Hoshina, K. Yamanouchi, and H. Nakano, *Chem. Phys. Lett.* **423**, 220 (2006).
- [11] K. Hoshina, Y. Furukawa, T. Okino, and K. Yamanouchi, *J. Chem. Phys.* **129**, 104302 (2008).
- [12] P. M. Kraus, M. C. Schwarzer, N. Schirmel, G. Urbasch, G. Frenking, and K. M. Weitzel, *J. Chem. Phys.* **134**, 114302 (2011).
- [13] N. Schirmel, N. Reusch, P. Horsch, and K.-M. Weitzel, *Faraday Discuss.* **163**, 461 (2013).
- [14] N. Kotsina, S. Kaziannis, and C. Kosmidis, *Chem. Phys. Lett.* **604**, 27 (2014).
- [15] Y. Boran, G. L. Gutsev, A. A. Kolomenskii, F. Zhu, A. Schuessler, and J. Strohaber, *J. Phys. B* **51**, 035003 (2018).
- [16] N. Ekanayake, M. Nairat, N. P. Weingartz, M. J. Michie, B. G. Levine, and M. Dantus, *J. Chem. Phys.* **149**, 244310 (2018).

- [17] T. Ando, A. Shimamoto, S. Miura, A. Iwasaki, K. Nakai, and K. Yamanouchi, *Commun. Chem.* **1**, 7 (2018).
- [18] N. Ekanayake, M. Nairat, B. Kaderiya, P. Feizollah, B. Jochim, T. Severt, B. Berry, K. R. Pandiri, K. D. Carnes, S. Pathak, D. Rolles, A. Rudenko, I. Ben-Itzhak, C. A. Mancuso, B. S. Fales, J. E. Jackson, B. G. Levine, and M. Dantus, *Sci. Rep.* **7**, 4703 (2017).
- [19] N. Ekanayake, T. Severt, M. Nairat, N. P. Weingartz, B. M. Farris, B. Kaderiya, P. Feizollah, B. Jochim, F. Ziaee, K. Borne, K. Raju P, K. D. Carnes, D. Rolles, A. Rudenko, B. G. Levine, J. E. Jackson, I. Ben-Itzhak, and M. Dantus, *Nat. Commun.* **9**, 5186 (2018).
- [20] E. Livshits, I. Luzon, K. Gope, R. Baer, and D. Strasser, *Commun. Chem.* **3**, 49 (2020).
- [21] K. Gope, E. Livshits, D. M. Bittner, R. Baer, and D. Strasser, *J. Phys. Chem. Lett.* **11**, 8108 (2020).
- [22] E. Wang, X. Shan, L. Chen, T. Pfeifer, X. Chen, X. Ren, and A. Dorn, *J. Phys. Chem. A* **124**, 2785 (2020).
- [23] Y. Zhang, B. Ren, C.-L. Yang, L. Wei, B. Wang, J. Han, W. Yu, Y. Qi, Y. Zou, L. Chen, E. Wang, and B. Wei, *Commun. Chem.* **3**, 160 (2020).
- [24] S. R. Gadre, S. D. Yeole, and N. Sahu, *Chem. Rev.* **114**, 12132 (2014).
- [25] E. Wang, X. Ren, W. Baek, H. Rabus, T. Pfeifer, and A. Dorn, *Nat. Commun.* **11**, 2194 (2020).
- [26] W. Klemperer and V. Vaida, *Proc. Natl. Acad. Sci. U.S.A.* **103**, 10584 (2006).
- [27] E. Herbst and E. F. van Dishoeck, *Annu. Rev. Astron. Astrophys.* **47**, 427 (2009).
- [28] A. G. G. M. Tielens, *Rev. Mod. Phys.* **85**, 1021 (2013).
- [29] E. S. Wirström, W. D. Geppert, A. A. Hjalmarsen, C. M. Persson, J. H. Black, P. Bergman, T. J. Millar, M. Hamberg, and E. Vigren, *Astron. Astrophys.* **533**, A24 (2011).
- [30] L. Campbell and M. Brunger, *Int. Rev. Phys. Chem.* **35**, 297 (2016).
- [31] F. J. Ciesla and S. A. Sandford, *Science* **336**, 452 (2012).
- [32] C. Meinert, I. Myrgorodska, P. de Marcellus, T. Buhse, L. Nahon, S. V. Hoffmann, L. L. S. d'Hendecourt, and U. J. Meierhenrich, *Science* **352**, 208 (2016).
- [33] P. Slavíček, B. Winter, L. S. Cederbaum, and N. V. Kryzhevoi, *J. Am. Chem. Soc.* **136**, 18170 (2014).
- [34] S. Xu, D. Guo, X. Ma, X. Zhu, W. Feng, S. Yan, D. Zhao, Y. Gao, S. Zhang, X. Ren, Y. Zhao, Z. Xu, A. Dorn, L. S. Cederbaum, and N. V. Kryzhevoi, *Angew. Chem., Int. Ed. Engl.* **57**, 17023 (2018).
- [35] J. Ullrich, R. Moshhammer, A. Dorn, R. Dörner, L. P. H. Schmidt, and H. Schmidt-Böcking, *Rep. Prog. Phys.* **66**, 1463 (2003).
- [36] X. Ren, T. Pflüger, M. Weyland, W. Y. Baek, H. Rabus, J. Ullrich, and A. Dorn, *J. Chem. Phys.* **141**, 134314 (2014).
- [37] X. Ren, E. Jabbour Al Maalouf, A. Dorn, and S. Denifl, *Nat. Commun.* **7**, 11093 (2016).
- [38] R. Car and M. Parrinello, *Phys. Rev. Lett.* **55**, 2471 (1985).
- [39] M. J. Frisch *et al.*, *Gaussian 16 Revision A.03* (Gaussian, Inc., Wallingford CT, 2016).
- [40] See Supplemental Material at <http://link.aps.org/supplemental/10.1103/PhysRevLett.126.103402> for further analysis on the proton transfer, electron transfer, rotational and vibrational energies of H_3^+ and $CH_3OH_2^+$ species, target temperature and additional ion-ion measurements on ethanol.
- [41] C. Richter, D. Hollas, C.-M. Saak, M. Förstel, T. Miteva, M. Mucke, O. Björneholm, N. Sisourat, P. Slavíček, and U. Hergenbahn, *Nat. Commun.* **9**, 4988 (2018).
- [42] B. Erk *et al.*, *Science* **345**, 288 (2014).
- [43] L. S. Cederbaum, J. Zobeley, and F. Tarantelli, *Phys. Rev. Lett.* **79**, 4778 (1997).
- [44] U. Hergenbahn, *Int. J. Radiat. Biol.* **88**, 871 (2012).
- [45] T. Jahnke, U. Hergenbahn, B. Winter, R. Drner, U. Frhling, P. V. Demekhin, K. Gokhberg, L. S. Cederbaum, A. Ehresmann, A. Knie, and A. Dreuw, *Chem. Rev.* **120**, 11295 (2020).
- [46] P. Linusson, M. Stenrup, A. Larson, E. Andersson, F. Heijkenskjöld, P. Andersson, J. H. D. Eland, L. Karlsson, J.-E. Rubensson, and R. Feifel, *Phys. Rev. A* **80**, 032516 (2009).
- [47] H. B. Schlegel, J. M. Millam, S. S. Iyengar, G. A. Voth, A. D. Daniels, G. E. Scuseria, and M. J. Frisch, *J. Chem. Phys.* **114**, 9758 (2001).
- [48] S. S. Iyengar, H. B. Schlegel, J. M. Millam, G. A. Voth, G. E. Scuseria, and M. J. Frisch, *J. Chem. Phys.* **115**, 10291 (2001).
- [49] H. B. Schlegel, S. S. Iyengar, X. Li, J. M. Millam, G. A. Voth, G. E. Scuseria, and M. J. Frisch, *J. Chem. Phys.* **117**, 8694 (2002).